2P

NASA TECHNICAL MEMORANDUM

NASA TM X-71992

COPY NO.

NASA TM X- 71992

(NASA-TM-X-71992) COMPRESSIVE STRENGTH OF FIBER REINFORCED COMPOSITE MATERIALS (NASA) 22 p HC $3.00 CSCL 11D

N74-31025

Unclas
G3/18 45780

24

COMPRESSIVE STRENGTH OF FIBER REINFORCED COMPOSITE MATERIALS

by John G. Davis, Jr.

Langley Research Center
Hampton, Virginia

TECHNICAL PAPER presented at the
ASTM - Composite Reliability Conference,
Las Vegas, Nevada, April 15-16, 1974

NATIONAL AERONAUTICS AND SPACE ADMINISTRATION
LANGLEY RESEARCH CENTER, HAMPTON, VIRGINIA 23665

24

1. Report No.	2. Government Accession No.	3. Recipient's Catalog No.
NASA TM-X 71992		

4. Title and Subtitle	5. Report Date
COMPRESSIVE STRENGTH OF FIBER REINFORCED COMPOSITE MATERIALS	August, 1974
	6. Performing Organization Code: 25.110
7. Author(s): John G. Davis, Jr.	8. Performing Organization Report No.
9. Performing Organization Name and Address: Materials Division, NASA - Langley Research Center, Hampton, VA 23665	10. Work Unit No.: 505-02-41-01
	11. Contract or Grant No.
12. Sponsoring Agency Name and Address: National Aeronautics & Space Administration, Washington, DC 20546	13. Type of Report and Period Covered: Technical Memorandum
	14. Sponsoring Agency Code

15. Supplementary Notes

Presented at ASTM - Composite Reliability Conference - April 15-16, 1974, Las Vegas, Nevada

16. Abstract

Results of an experimental and analytical investigation of the compressive strength of unidirectional boron-epoxy composite material are presented. Observation of fiber coordinates in a boron-epoxy composite indicates that the fibers contain initial curvature. Combined axial compression and torsion tests were conducted on boron-epoxy tubes and it was shown that the shear modulus is a function of axial compressive stress. An analytical model which includes initial curvature in the fibers and permits an estimate of the effect of curvature on compressive strength is proposed. Two modes of failure which may result from the application of axial compressive stress are analyzed, delamination and shear instability. Based on tests and analysis failure of boron-epoxy under axial compressive load is due to shear instability.

17. Key Words (Suggested by Author(s)) (STAR category underlined)	18. Distribution Statement
Composite materials, boron-epoxy, compressive strength, shear strength, shear modulus, nonmetallic materials	Unclassified - unlimited

19. Security Classif. (of this report)	20. Security Classif. (of this page)	21. No. of Pages	22. Price*
Unclassified	Unclassified		

*Available from { The National Technical Information Service, Springfield, Virginia 22151
STIF/NASA Scientific and Technical Information Facility, P.O. Box 33, College Park, MD 20740

COMPRESSIVE STRENGTH OF FIBER REINFORCED COMPOSITE MATERIALS

John G. Davis, Jr.
NASA-Langley Research Center
Hampton, Virginia

ABSTRACT: Results of an experimental and analytical investigation of the compressive strength of unidirectional boron-epoxy composite material are presented. Observation of fiber coordinates in a boron-epoxy composite indicates that the fibers contain initial curvature. Combined axial compression and torsion tests were conducted on boron-epoxy tubes and it was shown that the shear modulus is a function of axial compressive stress. An analytical model which includes initial curvature in the fibers and permits an estimate of the effect of curvature on compressive strength is proposed. Two modes of failure which may result from the application of axial compressive stress are analyzed, delamination and shear instability. Based on tests and analysis failure of boron-epoxy under axial compressive load is due to shear instability.

KEY WORDS: Composite materials, boron-epoxy, compressive strength, shear strength, shear modulus

INTRODUCTION

The behavior of unidirectionally fiber-reinforced composite materials when subjected to an axial compressive loading parallel to the fibers has been investigated both analytically and experimentally during the past decade. At the beginning of the study reported herein, an indepth review of the literature was conducted [1] and the following was evident:

(1) A unified theory for predicting compressive strength did not exist. (2) Data tended to support three possible modes of failure, delamination, microbuckling of the fiber, and fiber-matrix separation followed by microbuckling of the fiber. (3) A direct relationship between compressive strength and interlaminar shear strength had been noted for some materials. Study of these points led to postulation of an analytical model which allows microbuckling or delamination as potential failure modes and provided an explanation for the relationship between interlaminar shear and compressive strength. The model, analyses, and experiments performed to correlate the model with the behavior of boron-epoxy are discussed in the remaining portion of this paper.

SYMBOLS

A_m	cross sectional area of the m^{th} layer
a_o	amplitude of initial displacement, see figure 2.
b	width of beam
E_m	Young's modulus of the m^{th} layer
F_i	first moment of area of the i^{th} layer about the midplane
G	shear modulus of the composite
G_i	shear modulus of the i^{th} layer
G^*	apparent shear modulus of composite
h_i	thickness of the i^{th} layer
I_m	moment of inertia of the m^{th} layer about the midplane
L	length of laminate
n	total number of layers above the midplane
P_f	applied compressive load on the fiber layer

P_m	applied compressive load on the matrix or m^{th} layer
P_x	external shear load
P_z	external transverse load
P	applied compressive load on a beam
$\underline{P}_p$	load vector at the p^{th} node
$\underline{\underline{R}}_p, \underline{\underline{S}}_p, \underline{\underline{T}}_p$	submatrices that form part of the finite difference equations
U	the change in strain energy in going from the initial position to the buckled position
V_i	volume fraction of the i^{th} layer
W	work done by the applied load in going from the initial position to the buckled position
w_0	initial transverse displacement of the laminate
w_1	transverse displacement of the laminate due to bending and shear loads
w	total transverse displacement of the laminate
x,y,z	coordinates
$\underline{Y}_p$	solution vector for the p^{th} node point along the beam
γ_i	shear strain in the i^{th} layer of a multilayered media
δ	displacement of the applied axial force in going from the initial position to the buckled position
θ_i	angle between the z axis and the initial position of the cross section of the i^{th} layer
σ_c	compressive stress
σ_{cr}	applied compressive stress at which shear instability occurs
τ_i	shear stress in the i^{th} layer
$\tau_{m,m}$	interlaminar shear stress above the m^{th} layer and acting on the m^{th} layer

ϕ_i defined by $(\psi_i - \theta_i)$

ψ_i angle between the z axis and the final position of the deformed cross section of the i^{th} layer

ANALYTICAL MODEL

The model postulated herein is compared with the one used by Rosen [2] in figure 1. Each model is built-up from a series of hard and soft laminae. Rosen assumed that the laminae were initially straight and predicted two buckling modes, extension and shear. The advantages of the Rosen model are that strength is related to the matrix properties and the resulting equations are easy to use. As for disadvantages, predicted values are usually much larger than experimental measurements, fiber geometry is not taken into account and nonlinear behavior of the matrix is neglected.

The present model permits the laminae to contain initial curvature. As a consequence, under an increasing axial load the laminae undergo lateral deflection which induces interlaminar shear stress and may result in failure by delamination i.e., some of the early graphite-epoxy laminates. The second mode of failure considered is shear instability of the laminae. If the matrix material behaves in a nonlinear manner, the induced interlaminar shear stresses will cause the shear modulus of the composite to decrease and, correspondingly, the axial compressive stress at which shear instability occurs will decrease. Important features of the present model include:
(1) strength is related to constituent properties and geometry. (Both the fiber and matrix properties are taken into account. Filament size, initial curvature and collimation are reflected in the value of a_o and L.)
(2) An explanation for the relation between compressive and interlaminar

shear strengths is offered. (3) A decrease in shear modulus with increasing applied axial load is explained. The major disadvantage of the model is that it contains only two dimensions whereas the filamentary composite is a three dimensional material.

ANALYSIS

A brief description of the analysis utilized to predict interlaminar shear stress and shear instability in the analytical model follows. Complete derivations are presented in reference 1.

Interlaminar Shear Stress

A repeating element which consists of one fiber layer and two half layers of matrix material was analyzed as a multilayered Timoshenko beam loaded in axial compression (see figure 2). Each layer in the beam contains an initial transverse deflection, w_0, which can be represented by a sine wave. Both bending and shearing deformations are permitted in each layer. Since the beam represents a repeating element, the horizontal displacement, u, due to bending and shearing must vanish along the upper and lower surfaces in order to satisfy continuity of displacements. Subdividing the beam into 2n layers, taking into account symmetry about the midplane and applying the equations of equilibrium to each layer leads to the set of governing differential equations for the problem. Summation of moments yields:

$$\sum_{i=1}^{m} [E_i(I_i - F_i h_i)(\psi_i'' - \theta_i'') + E_i F_i \sum_{k=1}^{i-1} (h_{k+1} - h_k)(\psi_k'' - \theta_k'')]$$

$$- \sum_{i=1}^{m} G_i A_i(\psi_i - \theta_i + w_1') + h_{m+1} P_x/2$$

$$+ h_{m+1} \sum_{i=m+1}^{n} [E_i(F_i - A_i h_i)(\psi_i'' - \theta_i'') + E_i A_i \sum_{k=1}^{i-1} (h_{k+1} \tag{1}$$

$$- h_k)(\psi_k'' - \theta_k'')] = 0$$

Summation of vertical forces yields:

$$\sum_{i=1}^{n} G_i A_i w_1'' + \sum_{i=1}^{n} G_i A_i(\psi_i' - \theta_i') + P_z/2 - Pw'' = 0 \tag{2}$$

Continuity of displacements provides the remaining governing equation.

$$\phi_1 h_2 + \phi_2(h_3 - h_2) + \ldots + \phi_n(h_{n+1} - h_n) = 0 \tag{3}$$

Expressing the derivatives of ψ_i, θ_i, ϕ_i and w in terms of finite differences, dividing the beam into J intervals, and applying fixed-end boundary conditions permits one to transform equations (1) through (3) into the following set of matrix equations.

$$\begin{bmatrix} \underline{\underline{S}}_2 & \underline{\underline{T}}_2 & 0 & 0 & 0 & . & . & . \\ \underline{\underline{R}}_3 & \underline{\underline{S}}_3 & \underline{\underline{T}}_3 & 0 & 0 & . & . & . \\ 0 & \underline{\underline{R}}_4 & \underline{\underline{S}}_4 & \underline{\underline{T}}_4 & 0 & . & . & . \\ . & . & . & 0 & 0 & \underline{\underline{R}}_{J-1} & \underline{\underline{S}}_{J-1} & \underline{\underline{T}}_{J-1} \\ . & . & . & 0 & 0 & 0 & \underline{\underline{R}}_J & \underline{\underline{S}}_J \end{bmatrix} \begin{bmatrix} \underline{Y}_2 \\ \underline{Y}_3 \\ . \\ . \\ \underline{Y}_{J-1} \\ \underline{Y}_J \end{bmatrix} = \begin{bmatrix} \underline{P}_2 \\ \underline{P}_3 \\ . \\ . \\ \underline{P}_{J-1} \\ \underline{P}_J \end{bmatrix} \tag{4}$$

Considering the k^{th} node along the beam, the solution vector $\underline{Y}_k$ includes the rotation ϕ_i of each layer, the transverse deflection w_1 and the interlaminar shear stress which acts on the outer layers.

A computer program which utilizes the tridiagonal method of solution and had been written earlier by Swift [3] was modified to solve equations (4). The computer program increments the loading and adjusts the coefficient matrices as the loading is increased to account for nonlinear shear stress-strain behavior in the layers.

After the solution vectors are computed, interlaminar shear stresses may be computed by the following equation.

$$\tau_{m,m} = \frac{1}{bh_{m+1}} \left\{ \sum_{i=1}^{m} [E_i(I_i - F_i h_i)(\psi_i'' - \theta_i'') + E_i F_i \sum_{k=1}^{i-1} (h_{k+1} - h_k)(\psi_k'' - \theta_k'')] - \sum_{i=1}^{m} [G_i A_i(\psi_i - \theta_i + w_1')] \right\} \tag{5}$$

Equation (5) can be used to compute interlaminar shear stresses as a function of applied axial compressive stress. If the value of $\tau_{m,m}$ computed with equation (5) equals or exceeds the interlaminar shear strength of the composite material, failure will occur by delamination.

It will be shown herein that the axial compressive stress at which shear instability occurs is dependent on the shear modulus of each layer in the beam. The average shear stress in each layer can be computed as a function of axial compressive stress using the following equation

$$\tau_{ave} = \tau_{m,m} + \frac{E_m}{3}(h_{m+1} - h_m)^2(\psi_m'' - \theta_m'') + \frac{E_m}{2}(h_{m+1} - h_m) \sum_{i=1}^{m-1} (h_{i+1} - h_i)(\psi_i'' - \theta_i'') \tag{6}$$

Using values of shear stress computed by equation (6) and the shear stress strain curves for each material in the composite, the shear modulus of each layer can be computed as a function of axial compressive stress for subsequent use in the stability analysis.

Shear Stability

Figure 3 shows a segment of the multilayered beam used to represent the composite material. The length to width ratio of each layer is assumed to be small and thus bending is precluded. The magnitude of the applied end loads is such that a uniform axial strain is imposed. The repeating element is assumed to be symmetric about its midplane and compatibility of displacements along the boundaries is imposed. As a result, the average vertical displacement at the upper ends of the $+n^{th}$ and $-n^{th}$ layers will equal the displacement at the midplane of the repeating element. For convenience, the applied axial loads are replaced by a single load acting at the midplane of the repeating element.

The axial load which initiates shear buckling, may be calculated using an energy analysis, as indicated by Foye [4]. Referring to figure 3, it is noted that the work done by the external forces in going from the initial position to the buckled position is

$$W = P\delta \tag{7}$$

Noting

$$\delta = (1 - \cos w_1') \, dx \quad \text{and} \quad \cos w_1' \approx 1 - w_1'^2/2$$

equation (7) becomes

$$W = P \, w_1'^2 \, dx/2 \tag{8}$$

Since bending is precluded, the change in strain energy in going from the initial position to the buckled position is due only to shearing stresses and is given by

$$U = \sum_{i=1}^{n} \tau_i \gamma_i A_i \, dx \tag{9}$$

Expressing shear stress and strain in terms of displacement and rotations, equation (9) becomes

$$U = \sum_{i=1}^{n} G_i A_i \, (\phi_i + w_1')^2 \, dx \tag{10}$$

Equating W and U leads to

$$P w_1'^2 = 2 \sum_{i=1}^{n} G_i A_i \, (\phi_i + w_1')^2 \tag{11}$$

Equation (11), plus the following equation, which imposes continuity of displacements along the vertical edges of the repeating element, are the governing equations for predicting shear instability.

$$\sum_{i=1}^{n} A_i \phi_i = 0 \tag{12}$$

The minimum value of axial compressive load, P, which satisfies the governing equations can be determined using the method of Lagrange multipliers. Further, noting the relationship between axial load and stress and the definition of volume fractions, V_i, leads to the following equation for predicting the axial compression stress at which shear buckling occurs.

$$\sigma_{cr} = \frac{G_1 G_2 \ldots G_n}{V_1 G_2 \ldots G_n + V_2 G_1 G_3 \ldots G_n + \ldots + V_n G_1 \ldots G_{n-1}} \tag{13}$$

Shear moduli values substituted into equation (13) should be those corresponding to the average shear stresses induced by axial compression and calculated with equation (6). Neglecting to take into account the induced shear stresses and the corresponding reduction in shear modulus, equation (13) would predict the same value of axial stress for shear instability as given by Rosen [1] and Foye [4].

EXPERIMENT AND RESULTS

Fiber Curvature

The analytical model postulated herein is based on the assumption that the reinforcing fibers contain initial curvature. In order to verify that assumption, the coordinates of five arbitrarily selected fibers in a boron-epoxy laminate were measured (see figure 4). A 1.27 cm (0.50 in.) wide strip was machined from the central portion of a 15.24 cm (6.00 in.) wide by 10.16 cm (4.00 in.) long twelve ply laminate. The fibers were aligned in the length

direction of the strip. The strip was sliced into nominally 2.50 mm (0.10 in.) long coupons. Each slice across the strip removed approximately 1.78 mm (0.070 in.) of material. Thus the front faces of successive coupons were spaced at approximately 4.28 mm (0.170 in.) intervals. The length of each coupon was measured with a micrometer and the coordinates of the five fibers labeled in figure 4 were measured with a tool makers microscope.

Figure 5 shows typical results obtained from 22 cross sections along the length of the strip. Examination of the results for all fibers indicates: (1) Variation in the x coordinate was larger than in the y coordinate. (2) The fiber is skewed with respect to the z axis. (3) The fiber is essentially parallel to the x-z plane. (4) The fiber exhibits waviness along its length. Item (4) is perhaps the most important since it leads to the development of shear stresses when the fiber is compressed in the axial direction. As discussed earlier herein, the induced shear stresses can cause the composite to delaminate or reduce the shear modulus of the composite sufficiently to cause failure by shear instability.

Displacements ranging from 15.24 to 30.48 μm (0.0006 to 0.0012 in.) over a span of 0.864 cm (0.34 in.) were measured in the five fibers. Due to the irregular wave shape along each fiber, no attempt was made to express the displacement by a mathematical function. However, if segments of fibers are examined and the displacement equation shown in figure 2 is used, values of a_0/L required to fit the deflection range approximately from 0.0009 to .001875. As will be shown later herein, these deflections are sufficient to considerably influence the axial compressive strength.

Combined Compression and Torsion Test

In order to determine the influence of compressive stress on shear modulus, boron fiber uniaxially reinforced epoxy tubes were subjected to combined axial compression and torsion tests using the apparatus shown in figure 6. The specimen was mounted in series with a load cell and supported by a thrust bearing assembly. Compressive loading was applied by raising the lower platen, whereas torque was applied by attaching weights on two strings which connected to the moment arms. Magnitude of the applied torque was determined by measuring rotation of the lower end of the load cell with respect to the upper end. This rotation was measured with two direct current differential transformers (DCDT's). Diametrically opposite strain gage rosettes and a single strain gage located midway between the two rosettes were attached to the middle of the specimen.

Figure 7 shows shear stress-strain curves that were developed. During each test the axial stress was held constant at a predetermined value. The curves indicate that the initial slope which is equal to the apparent shear modulus ($G - \sigma$) decreases as the axial compressive stress increases. The initial slope of each curve shown in figure 7 is plotted as a function of applied compressive stress in figure 8. If the shear modulus of the composite, G, is assumed to be independent of axial compressive stress, the dashed curve represents the predicted behavior for the apparent shear modulus. Except for low values of compressive stress, the experimentally determined values of apparent shear modulus are less than those predicted by the dashed line. The difference increases with increasing values of compressive stress and thus indicates that shear modulus of the composite decreases with

increasing applied compressive stress. A curve, which intersects the abscissa at the highest compressive strength for boron-epoxy known to the author, has been drawn through the data. Based on the data shown it appears that the maximum compressive strength of boron-epoxy is limited by shear instability which occurs when the apparent shear modulus equals zero.

COMPARISON OF EXPERIMENT AND THEORY

Results from the combined compression and torsion tests were compared with computed results based on the interlaminar shear stress analysis. The boron-epoxy composite was modeled as shown in figure 9. The nonlinear shear stress-strain response of the epoxy matrix was calculated using the experimentally determined shear stress-strain curve for a boron-epoxy tube and assuming a stiffness in series model. Four values of initial deflection amplitude, a_o, were selected for use in the computations. The resulting values of a_o/L extended over the range of experimentally determined values reported herein.

A comparison of the experimental data and computed results is shown in figure 10. Examination of the figure and computations indicates: (1) Computed curves of apparent shear modulus as a function of axial compressive stress, based on assumed initial deflections corresponding to a_o/L equal to 0.001875 and 0.003750, bound the data reasonably well. (2) These values of a_o/L are of the same order of magnitude as the measured deflections reported herein. (3) Small initial deflections, $0.001875 \leq a_o/L \leq 0.003750$, reduce the axial compressive stress at which shear instability is predicted to occur from approximately 9.308 GPa (1350 ksi) to the range of 2.758 to 3.792 GPa (400 to 550 ksi). (4) Within the region bounded by $0.001875 \leq a_o/L \leq 0.00375$,

the maximum computed interlaminar shear stress was approximately 75.842 MPa (11,000 psi) which is less than the interlaminar shear strength of the boron-epoxy composite and indicates that failure was due to shear instability and not due to delamination. (5) Neglecting initial curvature in the fibers (assuming $a_o/L = 0$) as assumed in references [1] and [4], leads to a predicted value of compressive strength which is significantly higher than the experimentally determined value.

CONCLUSIONS

Experimental evidence that the fibers in a boron-epoxy composite contain initial curvature and that the shear modulus is a function of axial compressive stress was obtained. An analytical model which includes initial curvature in the fibers and which can be used to explain the observed behavior has been proposed. Two modes of failure, delamination and shear instability, were analyzed. Based on the test results and analysis, failure of the boron-epoxy under axial compressive loading is due to shear instability.

REFERENCES

[1] Davis, John G., Jr.: "Compressive Strength of Lamina Reinforced and Fiber Reinforced Composite Materials." PhD Thesis, Virginia Polytechnic Institute and State University, May 1973.

[2] Rosen, B. W.: "Mechanics of Composite Strengthening", Fiber Composite Materials, American Society of Metals, Metals Park, Ohio, October 1964.

[3] Swift, G. W.: The Solution of N Simultaneous Second Order Coupled Differential Equations by the Finite Difference Method. Dept. of Engr. Mech., Virginia Polytechnic Institute Report No. VPI-E-71-3. Contract No. DAA-F07-70-C-0444, February 1971.

[4] Foye, R. L.: Compressive Strength of Unidirectional Composites. AIAA Paper No. 66-143, January 1966.

[5] Suarez, J. A.; Whiteside, J. B.; and Hadcock, R. N.: The Influence of Local Failure Modes on Compressive Strength of Boron/Epoxy Composites. Composite Materials: Testing and Design. ASTM STP 497, February 1972, pp. 237-256.

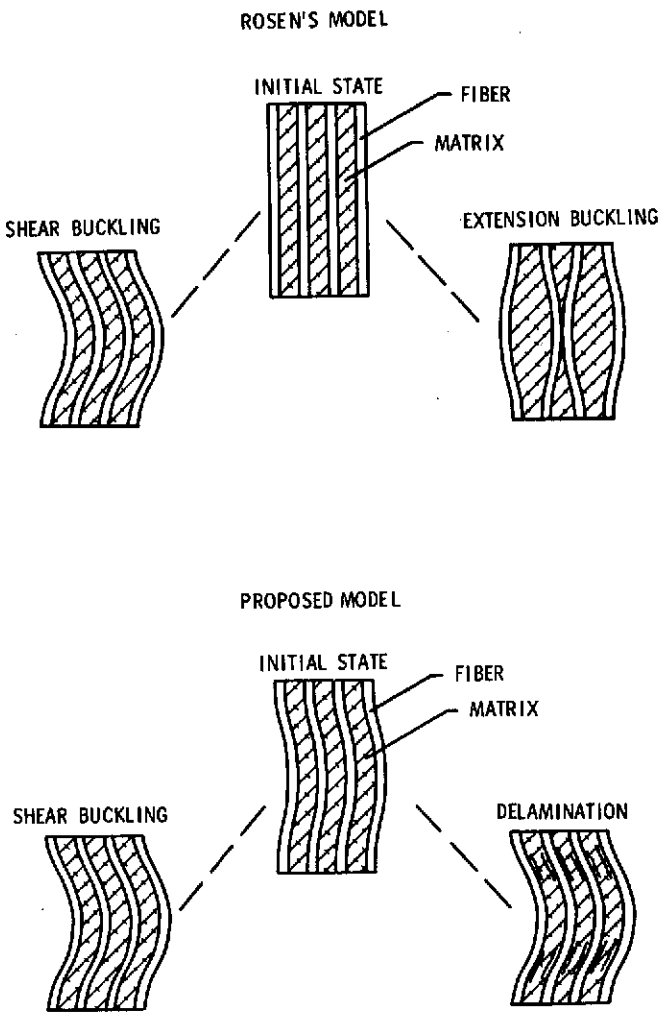

Figure 1.- Analytical model of fiber reinforced composite material.

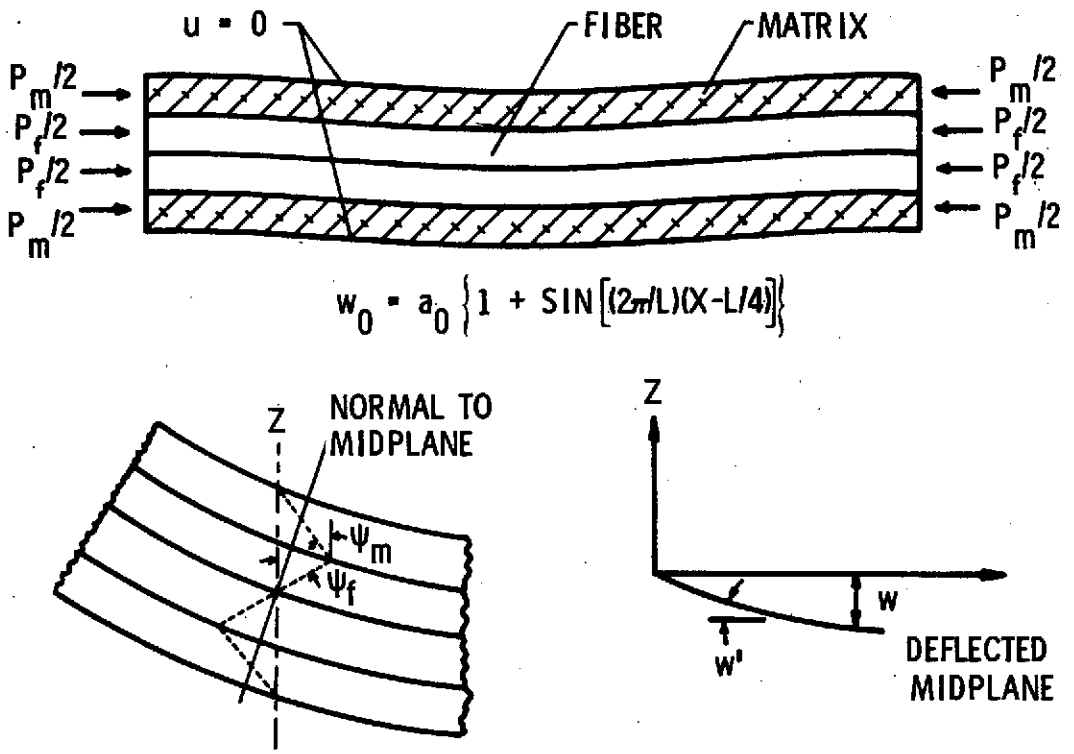

Figure 2.- Multilayered beam used in shear stress analysis of the composite material.

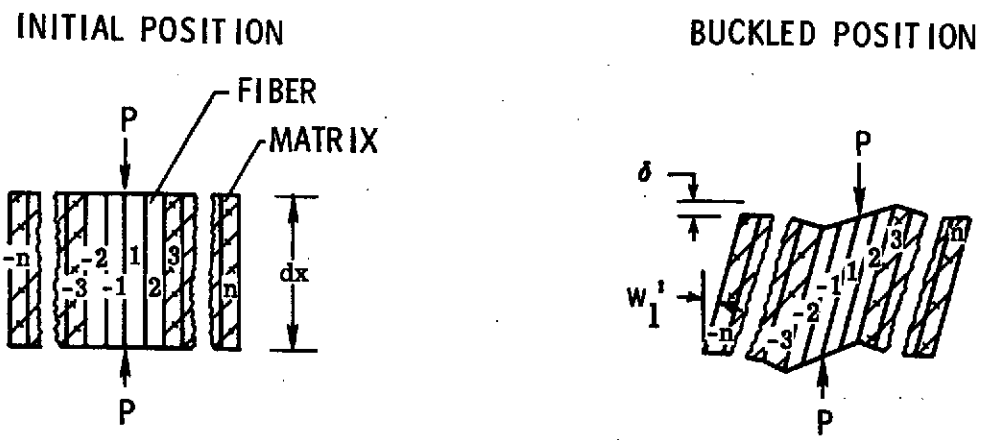

Figure 3.- Shear buckling of a multilayered beam.

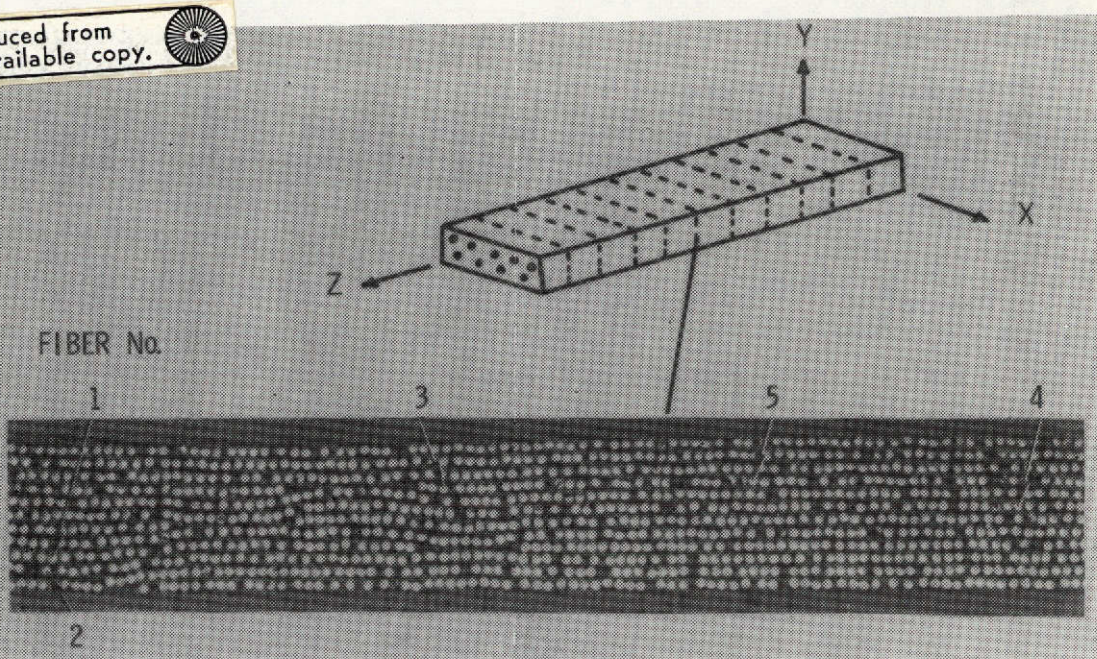

Figure 4.- Specimen sectioning to determine fiber coordinates.

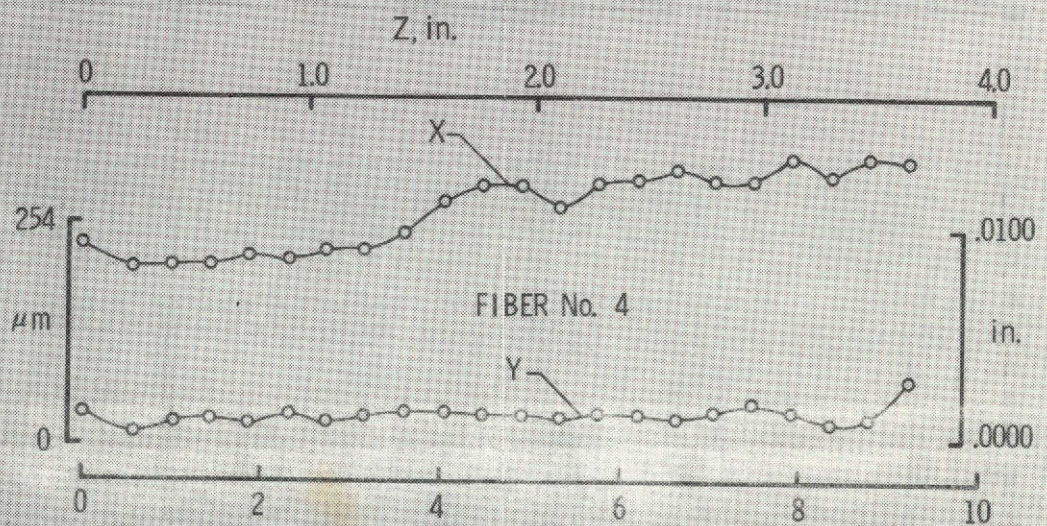

$$w_0 = a_0\left\{1 + \sin\left[(2\pi/L)(X - L/4)\right]\right\}$$

$1.524\ \mu m \leq a_0 \leq 3.048\ \mu m$
(.0006 in.) (.0012 in.)

$L = 1.73$ cm (.68 in.)

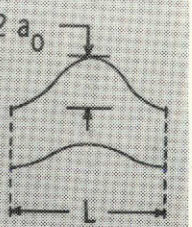

Figure 5.- Fiber coordinates.

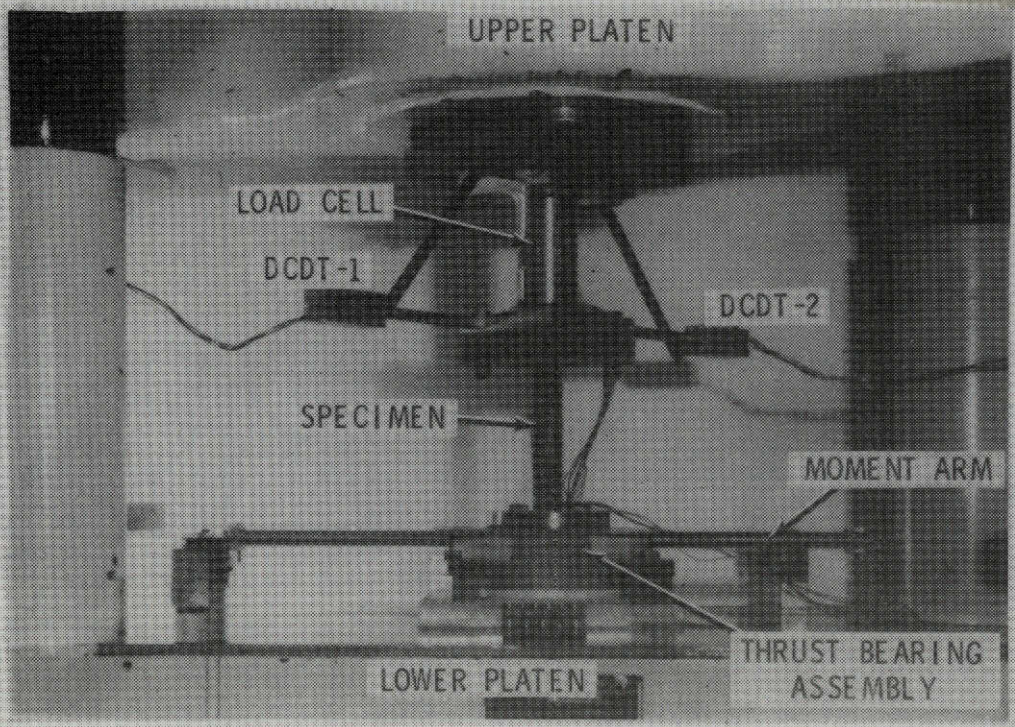

Figure 6.- Combined compression and torsion test of a boron-epoxy tubular specimen.

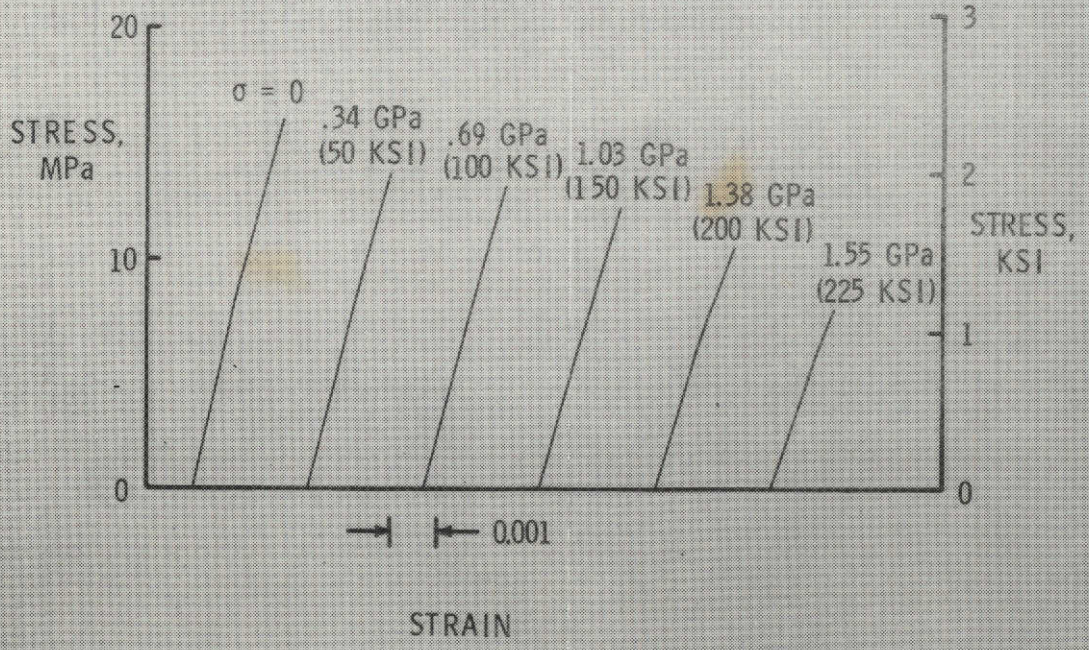

Figure 7.- Shear stress-strain plots for boron-epoxy.

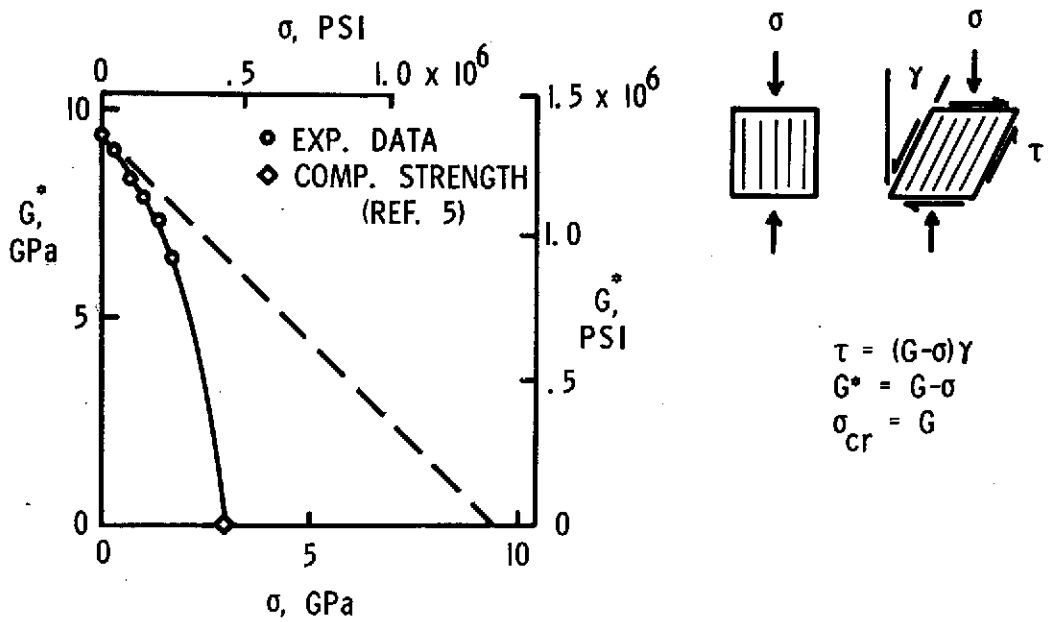

Figure 8.- Effect of compressive stress on the shear modulus of boron-epoxy.

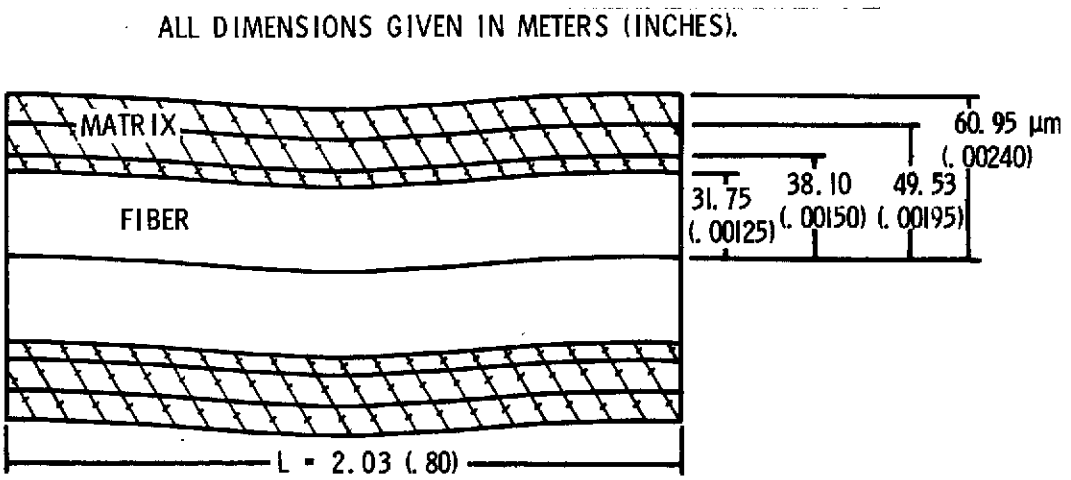

RANGE OF PARAMETERS INVESTIGATED

a_0 = 12.70 (.0005), 25.40 (.0010), 38.10 (.0015), 76.20 (.003) μm a_0/t = .2, .4, .6, 1.2

a_0/L = .000625, .001250, .001875, .003750

Figure 9.- Model used to simulate boron-epoxy in the stress analysis.

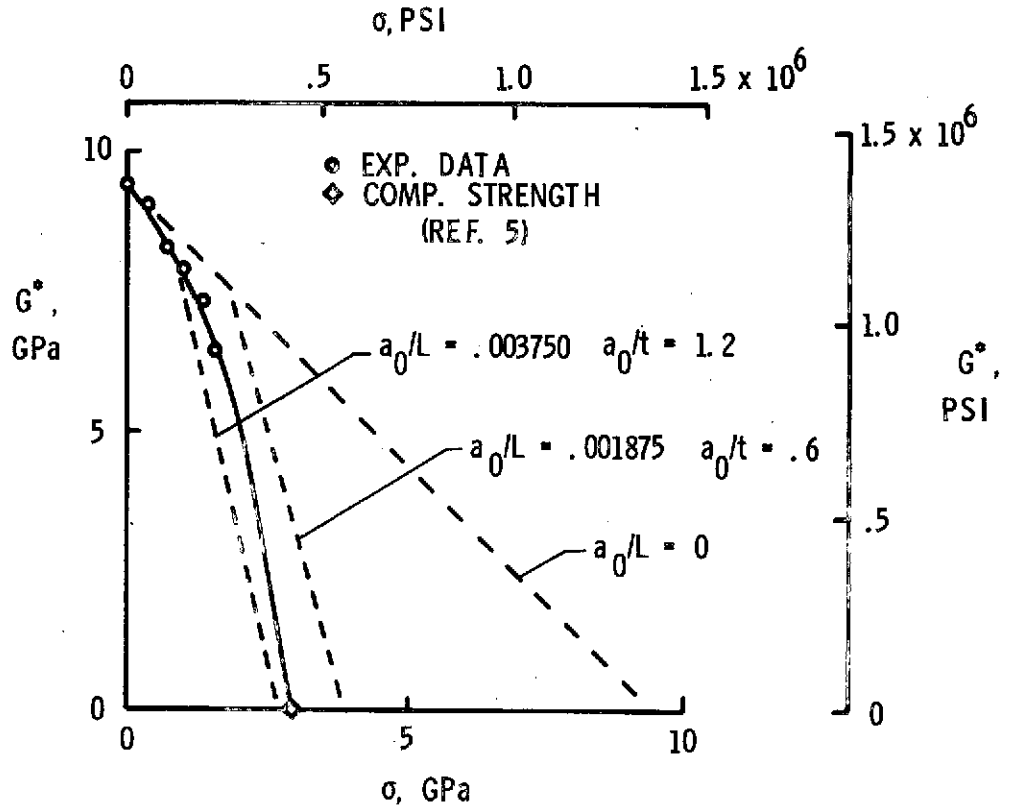

Figure 10.- Comparison of measured and predicted values of apparent shear modulus.